Journal of Applied Polymer Science

Preparation and characterization of composite hydrogels based on crosslinked hyaluronic acid and sodium alginate

Yong-Hao Chen,[1] Jun Li,[2] Yan-Bin Hao,[1] Jian-Xun Qi,[1] Ning-Guang Dong,[1] Chun-Lin Wu,[1] Qiang Wang[3]

[1]Institute of Forestry and Pomology, Beijing Academy of Agriculture and Forestry Science, Beijing 100093, China
[2]Beijing Institute of Landscape Architecture, Beijing 100102, China
[3]Institute of Agrofood Science and Technology, Chinese Academy of Agricultural Sciences, Beijing 100193, China
Correspondence to: Y. B. Hao (E-mail: jinhetaojht@263.net) and Q. Wang (E-mail: caaswq@163.com)

ABSTRACT: In this study, a novel composite hydrogel with improved cellular structure and mechanical properties was prepared by the crosslinking of hyaluronic acid (HA) and sodium alginate (SAL). The amide linkages (covalent bonds) in the hydrogel that we expected to form were confirmed by Fourier transform infrared spectroscopy. The hydrogels had a pore size larger than 100 μm and were observed by scanning electron microscopy. Texture profile analysis indicated that the hardness of the hydrogels was enhanced by an increase in the polymer's concentration, but it declined with an increase in the HA/SAL molar ratio. The swelling capacity was reduced with increases in the polymer's concentration and the 1-ethyl-3-(3-dimethyl aminopropyl)-1-carbodiimide hydrochloride (EDC)/HA molar ratio, and it was enhanced by an increase in the HA/SAL molar ratio. The resistance against hyaluronidase was negatively correlated with the proportion of HA in the hydrogels and positively correlated with the EDC/HA molar ratio. Given the improved physicochemical properties that we produced, these novel hydrogels may have the potential to be applied in tissue engineering scaffolding. © 2015 Wiley Periodicals, Inc. J. Appl. Polym. Sci. **2015**, *132*, 41898.

KEYWORDS: crosslinking; gels; polysaccharides

Received 18 July 2014; accepted 9 December 2014
DOI: 10.1002/app.41898

INTRODUCTION

Hyaluronic acid (HA) is a linear, unbranched acid mucopolysaccharide consisting of alternating *N*-acetyl-D-glucosamine and D-glucuronic acid. In an extracellular matrix, HA is the backbone of glycosaminoglycan superstructure complexes,[1] and it is widely distributed throughout the body. Moreover, it is a major component of synovial fluid and is a chondro-inductive agent.[2] During the process of embryogenesis, HA can affect cell migration and differentiation, and it can also regulate the constituent extracellular matrix. Because of its nonimmunogenicity, HA is easily recognized by specific surface receptors of various cells during the tissue repair process. HA promotes the migration and differentiation of mesenchymal cells and epithelial cells and facilitates collagen deposition and vasculogenesis.[3] Thus, it is an attractive building block with applications in orthopedic surgery for the treatment of osteoarthritis,[4] postsurgical antiadhesion,[5] and tissue engineering.[6,7]

HA is an ideal material for tissue engineering. Using HA, we prepared a hydrogel with potential applications for cartilage scaffolding, and we describe it in this article. However, HA hydrogels have poor mechanical properties that restrict their applications in tissue engineering.[8] Furthermore, single HA hydrogels cannot form a porous microstructure, which is necessary to provide space and mechanical support for tissue growth.[9]

Additionally, HA has a higher swelling capacity because of its strong hydrophilicity; this swelling capacity can influence the figure and morphology of the hydrogel and the cell growth. To obtain an optimal hydrogel, it is necessary to modify the natural polymers physically or chemically. Some strategies for the modification of HA through carboxyl and hydroxyl groups have been developed to improve its mechanical properties while maintaining its natural biocompatibility and nonimmunogenicity.[10] The chemical modification methods to produce HA derivatives include crosslinking, grafting, esterification, and composite modification.

Presently, composite modification is attracting more and more attention because of its unique advantage in which the composite hydrogels may combine the merits of the two original molecules.[11]

Table I. Prepared Samples of Hydrogels with Different Concentrations, Molar Ratios of HA to SAL, and Molar Ratios of EDC to HA

Samples I[a]	Concentration (%)	Samples II[b]	*X*	Samples III[c]	*Y*	EDC (mmol/L)
C1	0.5	P1	4	E1	2	16.66
C2	1.0	P2	2	E2	4	33.32
C3	1.5	P3	1	E3	6	49.98
		P4	0.5	E4	8	66.64
		P5	0.25	E5	10	83.30
				E6	12	99.96

X, molar mass of HA repeating units per molar mass of SAL repeating units; *Y*, molar mass of EDC repeating units per molar mass of HA repeating units.
[a] C1–C3: The *X* value was 0.5, and the amount of EDC was 20.55 mmol/L.
[b] P1–P5: The final concentration of both polymers was 1.0%, and the amount of EDC was 20.55 mmol/L.
[c] E1–E5: The final concentration of both polymers was 1.0%, and the *X* value was 0.5.

To improve HA's poor mechanical properties, retain its swelling capacity, and form a microstructure with a certain pore size, HA was crosslinked with sodium alginate (SAL) to form the novel hydrogels described in this article. SAL, a linear anionic polysaccharide of (1,4)-linked α-L-guluronate and β-D-mannuronic acid residues,[12] is a carbohydrate-derived natural polymer that is used in a variety of applications, including food processing, drug transmission,[13] and the creation of three-dimensional cultures of specific cells.[14] Its capacity for gelatinization is greatly increased by the presence of divalent ions such as Ca^{2+}, which can be created by carboxylate groups of alginate in a tetradentate structure with the well-known egg-box model.[15]

Compared with HA hydrogels, SAL hydrogels generally have good mechanical properties. Therefore, SAL was selected to be crosslinked with HA; this was done to offer more compression strength for the hydrogel once the composite hydrogel was formed. SAL is also a natural polysaccharide with good biocompatibility.[16] Additionally, the SAL hydrogel can facilitate the proliferation of cartilage cells *in vitro* and *in vivo*,[17] and it can be used as a carrier of injectable chondrocyte.[18] Furthermore, the chemical association of SAL with other polysaccharides, such as chitosan[15] and chondroitin sulfate,[19] has been reported. The preparation of a hydrogel with HA and SAL was also presented recently. Ganesh *et al.*[20] developed an injectable composite gel enzymatically crosslinked by HA and alginate, which were prepared via the oxidative coupling of tyramine-modified sodium alginate and sodium hyaluronate in the presence of horse radish peroxidase and hydrogen peroxide (H_2O_2). The results show that it was feasible to develop covalently crosslinked hydrogels through composite modification. However, this injectable composite gel could not be applied in tissue engineering scaffolds because of its physical and mechanical properties. Dahlmann *et al.*[21] prepared a fully defined *in situ* hydrogelation system based on HA and alginate in which aldehyde and hydrazide derivatives enabled the covalent hydrazone crosslinking of polysaccharides in the presence of viable myocytes. This *in situ* crosslinking hydrogel represents a valuable toolbox for the fine tuning of engineered cardiac tissue. Oerther *et al.*[22] prepared a kind of alginate–hyaluronate mixture and investigated its rheological properties. However, the alginate–hyaluronate mixture was simply a mixed solution of the two polymers; no covalent bonds formed. Also, that mixture was meant for surgical applications, and only its rheological behavior and viscosity were measured. Chung *et al.*[14] fabricated a porous HA/SAL scaffold based on an interpenetrating polymeric network technique, in which HA and SAL were crosslinked with poly(ethylene glycol) diglycidyl ether and calcium chloride, respectively. Additionally, Coates *et al.*[23] reported photocrosslinked SAL hydrogels and demonstrated the utility of the hydrogels, which were interpenetrated HA chains used to support stem cell chondrogenesis. Although HA was added to the photocrosslinked scaffolds and upregulated gene markers, SAL and HA were still not crosslinked by covalent crosslinks.

In this study, the combination of HA and SAL was chemically crosslinked with 1-ethyl-3-(3-dimethyl aminopropyl)−1-carbodiimide hydrochloride (EDC) as the carboxyl-activating agent and adipic dihydrazide (ADH) as the crosslinker. A series of hydrogels with improved physicochemical properties, which had potential applications in tissue engineering, was expected to be obtained. The hydrogels might have the merits of the two original molecules. On the one hand, the porous microstructure and resistance to hyaluronidase (HAase) was improved through the crosslinked structure. On the other hand, the mechanical properties and texture profile characteristics of the hydrogels were enhanced. In this article, we report the preparation and characterization of these HA–SAL hydrogels.

EXPERIMENTAL

Materials

HA, with an average molecular weight of 1.5×10^6 Da and produced by a *Streptococcus*, was supplied by Novozymes (Denmark) as a dry powder. SAL powder with 200-mesh screen granularity was contributed by Jingyan Co., Ltd. (Qingdao, China) and confected into a 10 mg/mL aqueous solution with a viscosity of 205 mPa s at 25°C. EDC was purchased from Gongjia (Shanghai, China). ADH was contributed by Jinyuan Co., Ltd. (Beijing, China), and HAase (EC 3.2.1.35, 999 U/mg of solid) was purchased from Sigma. Acetate buffer solution (0.2 mol/L, pH 3.6) and 3.7 mL of 0.2 mol/L sodium acetate was mixed with 46.3 mL of 0.2 mol/L acetic acid.

Preparation of the HA–SAL Hydrogels

As shown in Table I, a series of HA–SAL hydrogel samples based on different final concentrations (weight/volume) of HA

and SAL, different molar ratios of repeating units of HA and SAL, and different amounts of EDC, respectively, was prepared. First, both HA and SAL were dissolved in 50 mL of distilled water. After complete dissolution, adequate ADH was added to the mixed solution, and the pH was adjusted to 4.75 ± 0.05 by the addition of an acetate buffer solution and then the addition of EDC. The mixed solution was stirred under an optimal rotating speed at room temperature for 4 h, and the pH was maintained at 4.75 ± 0.05 by the addition of acetate buffer solution during the reaction process. To remove the residual ADH and EDC in the hydrogels, the purification process was performed by several washes with double distilled water and then kept at 4°C.

Characterization of the HA–SAL Hydrogels

Fourier Transform Infrared (FTIR) Spectroscopy Analysis. The prepared hydrogels were lyophilized and analyzed with FTIR spectroscopy (Nicolet Nexus, Thermo Electron) with the KBr pellet method in the range 4000–400 cm^{-1} to confirm the formation of amide bonds.

Scanning Electron Microscopy (SEM) Characterization. After the hydrogels were lyophilized, their microstructures were observed with SEM (Hitachi SEM-2500, Japan) after the hydrogels were coated in gold with an ion coater.

Texture Profile Analysis (TPA). The characterization of the texture profile of the prepared hydrogels was investigated with TPA (Cns-Farnell, Britain). The hydrogels were put into an aluminum specimen box with a diameter of 5 cm, and an A/BE35 aluminum probe was used. The test consisted of the compression of 3 cm^3 of the hydrogel two times in a reciprocating motion with the following parameters: a pretest speed of 2.0 mm/s, a test speed of 0.8 mm/s, a posttest speed of 2.0 mm/s, a rupture test distance of 4.0%, a distance of 50%, and a temperature of 25°C.

Swelling Capacity of the Hydrogels. The lyophilized hydrogels with known weight were immersed in distilled water at 37°C for 12 h. After the excess water was removed from the surface with two pieces of dry paper, the samples were reweighed. The retention rate of the hydrogels (q) was calculated according to eq. (1):

$$q = W^*/W \tag{1}$$

where W^* represents the equilibrium swollen weight (g) and W is the weight of the lyophilized sample (g). The reported data is the average of three samples.[11]

Resistance of the Hydrogels Against HAase *In Vitro*. The *in vitro* degradation of the prepared hydrogels was determined through the incubation of the sample with HAase at 37°C according to the methods of Liu *et al.*[11] with a slight modification. Solid samples of HA–SAL hydrogels were dissolved in 10 mL of HAase solution with an enzyme activity of 10 U/mL. At 3-h intervals, 1 mL of supernatant was taken from the reaction system, and 1 mL of fresh HAase solution was supplemented. The collected supernatant samples were precipitated with 2.5 mL of absolute ethanol. After centrifugation at 12,000 rpm and 4°C for 10 min, the precipitate was diluted with 20 mL of distilled water. The content of HA was analyzed with the cetyltrimethyl ammonium bromide (CTAB) turbidimetric method.[24] The percentage degradation was calculated by the division of the amount of HA released at a given time point by the final amount of HA collected when the concentration of HA in the solution was constant. At a given time point i, the weight of released HA (W_i) was calculated according to eq. (2):

$$W_i = C_i V + \sum C_{i-1} V_s \tag{2}$$

where C_i and C_{i-1} are the concentrations of released HA (mg/mL) in the solution at time i and $i-1$, respectively; V is the total volume of the solution (10 mL); and V_s is the volume of the sample (1 mL).

Statistical Analysis

Statistical evaluations were performed by F tests to evaluate the differences among the experimental groups. A value of $p < 0.05$ was considered significant.

RESULTS AND DISCUSSION

Preparation of the HA–SAL Hydrogels

In this study, we prepared and characterized new hydrogels based on HA chemically crosslinked with SAL. As shown in Figure 1, both HA and SAL offer carboxyl groups, and ADH provided amidogen groups. As a water-soluble carbodiimide, EDC was used as a crosslinking agent because of its well-known ability to link HA with amine.[11,25] In the reaction, EDC changed into a water-soluble urea derivative, which has been proven to be nontoxic[26] and could be removed easily because of its water solubility. The crosslinking reaction scheme is shown in Figure 1(c) and can be summarized as follows. First, EDC reacted with carboxyl groups to form an unstable intermediate *O*-acylisourea. In the absence of nucleophiles, the unstable intermediate *O*-acylisourea could be rearranged to a stable *N*-acylurea, whereas in the presence of nucleophiles such as amines, the unstable intermediate *O*-acylisourea might form an amide linkage between the amine and the acid because of nucleophilic attack.[25] In this reaction, the nucleophile was ADH, which supplied amines. Additionally, the reaction between EDC and carboxyl groups depended on the pH, and the optimal pH ranged from 4.0 to 5.0. In this study, we hypothesized that the carboxyl groups of both SAL and HA could react with EDC and form amide linkages with ADH. Thus, SAL and HA were crosslinked through ADH. Of course, under certain conditions, the reaction might occur between or inside the same molecules and form HA–HA crosslinks or SAL–SAL crosslinks. This possible reaction is shown in Figure 1. As shown in Table I, the HA–SAL hydrogels were synthesized with different concentrations and molar ratios of HA to SAL and different amounts of EDC.

FTIR Spectra of the HA, SAL, and HA–SAL Hydrogels

To obtain information about the structure of the chemical linkages between HA and SAL, FTIR spectroscopy was performed on HA, SAL, and all of the obtained hydrogels after they were purified and lyophilized. Figure 2 shows the FTIR spectra of the native HA, SAL, and HA–SAL hydrogels. The principal differences in the FTIR spectra between the initial polymers and the HA–SAL hydrogel were as follows: assigned to carboxyl groups, both HA and SAL peaked at about 1410 cm^{-1} (ν_s COO^-) and also at 1617 cm^{-1} (ν_{as} COO^-). However, when the hydrogel

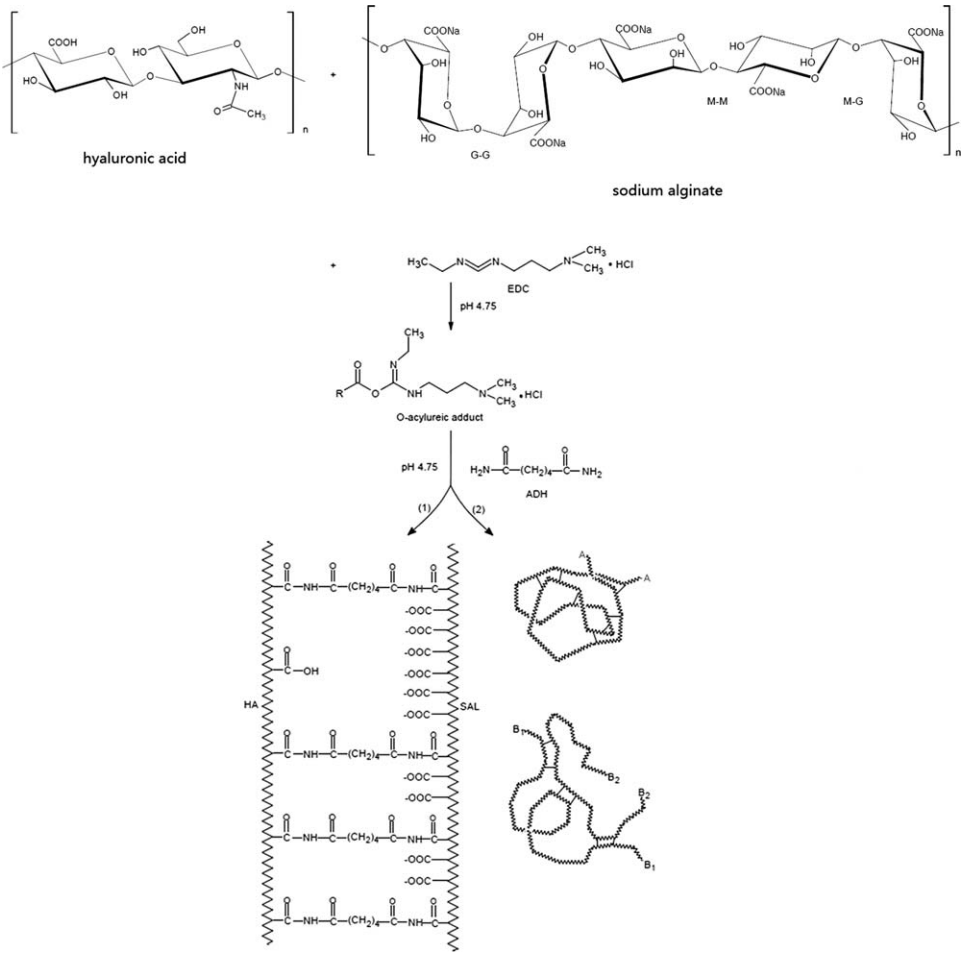

Figure 1. Chemical structures of (a) HA and (b) SAL and (c) schematic representation of the formation of HA–SAL hydrogels.

formed, the peaks at 1410 and 1617 cm^{-1} disappeared. Instead, there was an intense peak at 1644 cm^{-1} associated with amide bonds in the HA–SAL hydrogel. This was the product of the reaction between the carboxyl groups and the amidogen groups of ADH. Additionally, the relative peak sharpness at about 3420 cm^{-1} of the HA–SAL hydrogel fell between those of HA and SAL because of the introduction of amine links. Therefore, the hypothesis that HA and SAL were crosslinked by ADH with EDC as the carboxyl-activating agent was supported and confirmed.

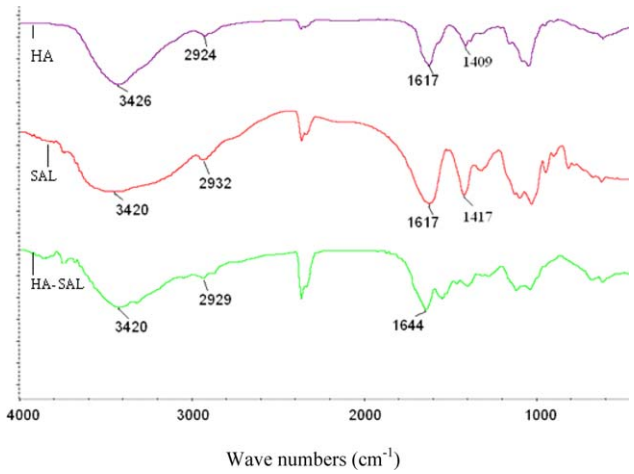

Figure 2. FTIR spectra of the HA, SAL, and HA–SAL hydrogels. [Color figure can be viewed in the online issue, which is available at wileyonlinelibrary.com.]

SEM Characterization of HA–SAL Microstructure

The prepared hydrogels with different molar ratios of HA and SAL were lyophilized and investigated by SEM. The obvious difference in microstructure between the hydrogels is shown in Figure 3. The HA hydrogel [Figure 3(a)] consisted of a filiform texture, and no porous structure formed, whereas the SAL hydrogel [Figure 3(f)] was a honeycomb structure with pore sizes between 30 and 80 μm. Scaffolds for cartilage tissue engineering must have a highly porous and interconnected pore structure to ensure a biological environment that is conducive to cell attachment and proliferation, tissue growth, and the passage of nutrient flows.[27–29] Only a pore size greater than 100 μm provides sufficient space for cell growth.[30] Hydrogels formed by a single molecule are not suitable for tissue scaffolding. However, the composite HA/SAL hydrogels demonstrated

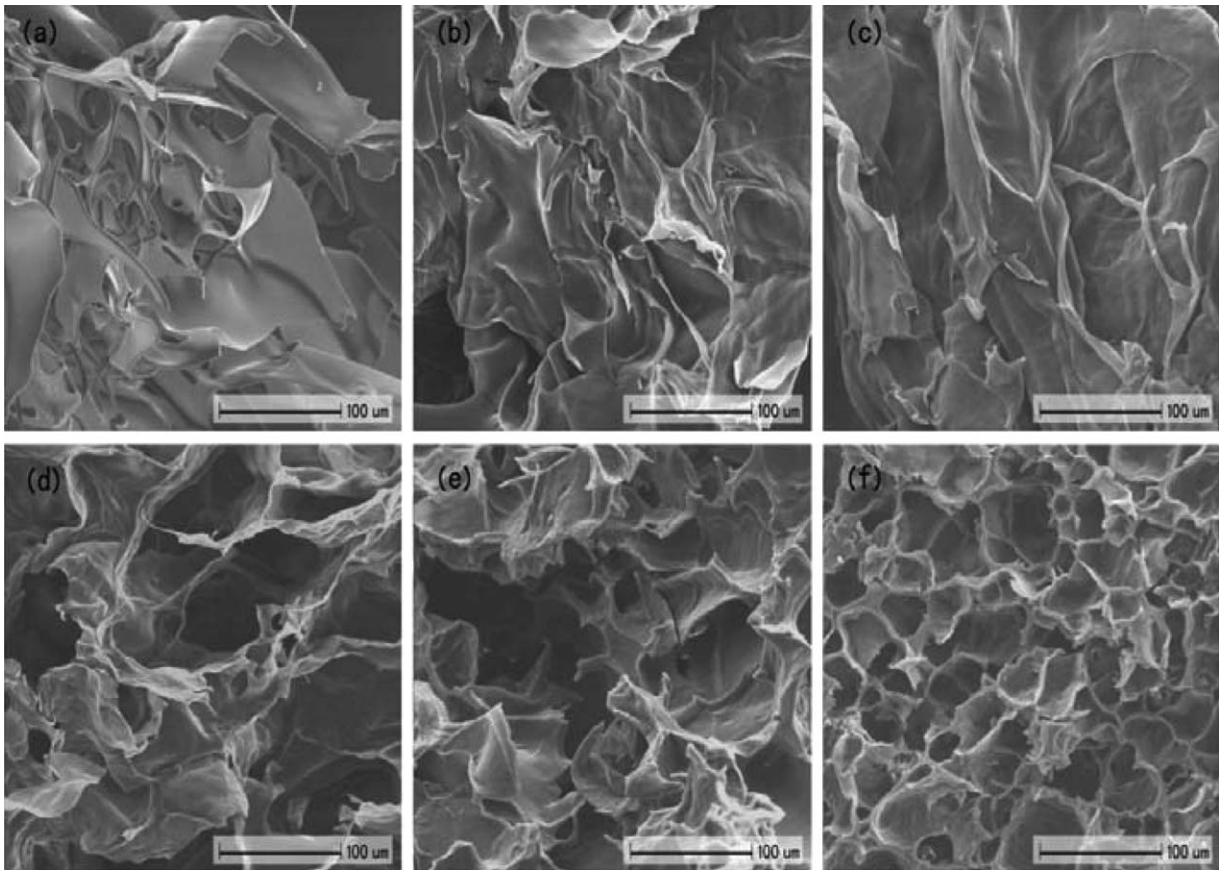

Figure 3. SEM micrographs of hydrogels with different molar ratios of HA to SAL at 15 kV (bar = 100 μm): (a) HA hydrogel, (b) 4:1 HA/SAL (P1), (c) 1:1 HA/SAL (P3), (d) 1:2 HA/SAL (P4), (e) 1:4 HA/SAL (P5), and (f) SAL hydrogel.

that the microstructures of the hydrogel depended on the proportions of HA and SAL. Figure 3(b–e) indicates that with increasing SAL, more and more porous microstructures appeared in the hydrogels, whereas with the increase of HA, laminated structures were increasingly formed. As shown in Figure 3(d), when the molar ratio of HA to SAL was 1:2 (P4), a relatively regular porous network could be observed, and the mean pore size was higher than 100 μm, which was suitable for the viability and differentiation of chondrocytes.[31]

TPA

The balance between the material porosity and mechanical strength is one of the major challenges in the development of load-bearing scaffolds for cartilage tissue engineering. A highly porous structure is preferred for cell growth and proliferation; however, porosity is achieved at the expense of mechanical strength.[14] As shown in the SEM characterizations, the composite hydrogel obtained a suitable pore structure, which met the requirements for scaffolding; scaffolds for cartilage tissue engineering must have enough mechanical strength to support cartilage tissue regeneration at the site of implantation and maintain sufficient integrity during both *in vitro* and *in vivo* cell growth.[27–29]

Although there is no clearly defined criterion for the mechanical properties required by cartilage tissue engineering, many researchers, such as Chung *et al.*,[14] selected compressive strength to evaluate the mechanical strength of a scaffold. In this study, texture characteristics were adopted to indicate the mechanical properties of the prepared hydrogels. The texture characteristics, including hardness, fracturability, springiness, and cohesiveness were investigated and are illustrated in Figure 4. Figure 4(a) shows that in a TPA test, a standard-sized sample was compressed in a reciprocating motion, and the typical force–time curve that results with two compression cycles is described in Figure 4(b). As one main measure of TPA, *hardness*, which is associated with compressive strength, indicates the resistance produced by the hydrogel surface when another object is pressing into it, and it is defined as the maximum peak force during the first compression cycle [Figure 4(c)]. As shown in Figure 4(c), the *fracturability* is defined as the force at the first significant break in the TPA curve, and it can be measured as the ease with which the material fractures under an increasing compression load. Springiness is related to the height that the material recovers during the time that elapses between the end of the first compression and the start of the second compression. The TPA macro collects this parameter and calculates the value as the time difference between points 4 and 5 divided between the time difference between points 1 and 2, as shown in Figure 4(c). There are no units for this parameter. *Cohesiveness* is defined as the ratio of the positive force area during the second compression to that during the first compression and is the value calculated as the area between points 4 and 6 divided by the area between points 1 and 3, as shown in Figure 4(d). The

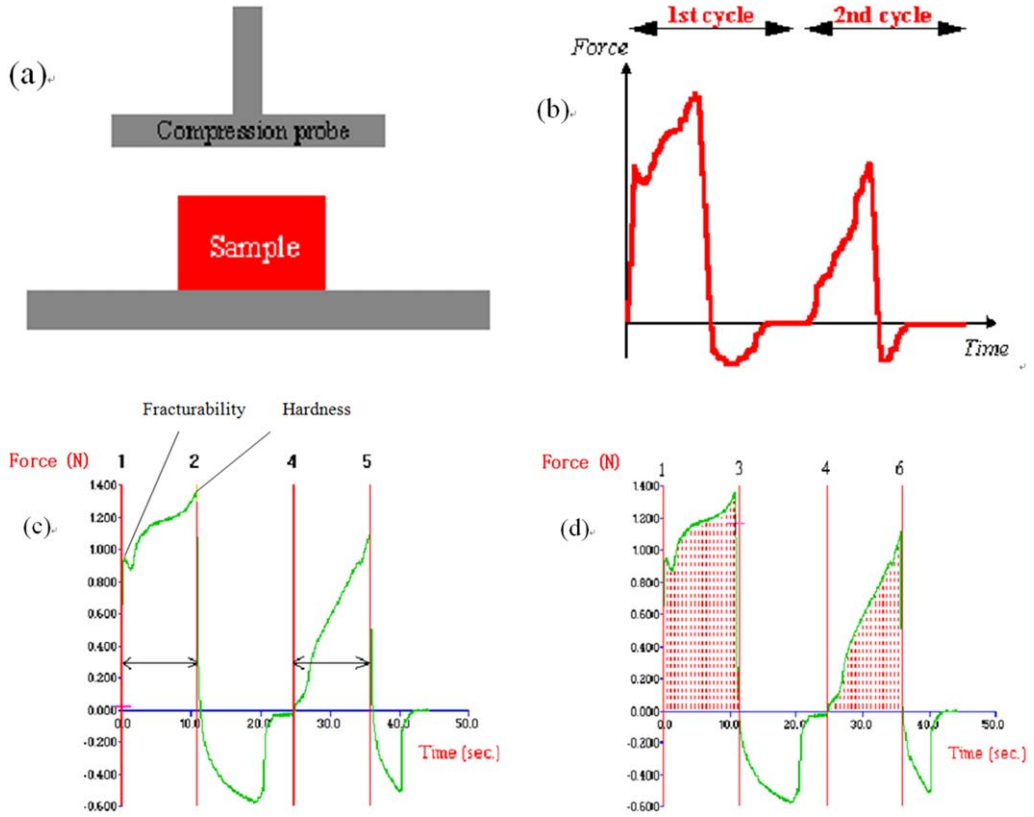

Figure 4. Typical TPA curve and illustration of the textural parameters: (a) texture analyzer setup; (b) typical Texture Expert curve; (c) typical Texture Expert TPA plot highlighting the source of the hardness parameter, fracturability parameter, and springiness parameter; and (d) typical Texture Expert TPA plot highlighting the source of the cohesiveness parameter. [Color figure can be viewed in the online issue, which is available at wileyonlinelibrary.com.]

cohesiveness may be measured as the rate at which the material disintegrates under mechanical action. There are no units for this parameter either.

All of the texture characteristics mentioned previously and their measured values indicate different profiles of the mechanical properties of the hydrogels. As shown in Table II (C1–C3), the hardness and fracturability of the hydrogels correlated positively to the final concentrations (weight/volume) of HA and SAL. A greater hardness or compressive strength could provide sufficient support for cell growth *in vitro* and *in vivo*. However, the springiness and cohesiveness at lower concentrations were slightly higher than those at high concentrations of HA and SAL. Cohesiveness is advantageous for cell attachment in the early stage, so the concentration of HA should be controlled and adjusted according to the demands placed on the hardness and cohesiveness of the tissue scaffold.

Table II (P2–P4) also shows that the hardness of the hydrogels was enhanced with the increase of SAL in the hydrogels. The fracturability, springiness, and cohesiveness reached higher values when the HA/SAL molar ratio reached 0.5 (P4). This indicates that SAL could increase the hardness, fracturability, springiness, and cohesiveness, which are important properties for hydrogels used as scaffolding materials. The hardness of the hydrogel (P4) in this study reached 184 g and had a cohesiveness of 0.557; these values were similar to those of the HA hydrogels (C2); meanwhile, the study hydrogel had a better pore structure. These qualities make this hydrogel attractive for use as a cartilage tissue engineering scaffold material.

Additionally, Table II (E1–E6) indicates that the hardness and fracturability were significantly affected by the EDC/HA molar

Table II. Characterization of the Texture Profiles of Different Hydrogel Samples

Sample	Hardness (g)	Fracturability (g)	Springiness	Cohesiveness
C1	70.76	59.19	0.985	0.536
C2	184.00	157.77	0.987	0.557
C3	256.86	201.09	0.925	0.516
P2	129.03	106.81	0.974	0.523
P3	137.11	93.74	0.961	0.468
P4	184.00	157.77	0.987	0.557
E1	11.34	10.04	0.912	0.454
E2	74.15	63.87	0.955	0.552
E3	357.06	253.56	0.961	0.493
E4	354.60	158.70	0.928	0.395
E5	437.75	232.29	0.913	0.381
E6	344.07	162.01	0.821	0.316

ratio. The hardness increased with the EDC/HA molar ratio and reached the highest value, 437.75 g, when the EDC/HA molar ratio was 10 (E5). The fracturability and springiness achieved peak values of 253.56 g and 0.961, respectively, when the EDC/HA molar ratio was 6 (E3). The cohesiveness presented a trend of first rising and then decreasing. Meanwhile, the peak appeared at E2 when the EDC/HA molar ratio was 4:1. The increasing use of EDC could have enhanced the crosslinking density and improved the texture profile to some extent. However, excessively high EDC/HA molar ratios might have caused overly rapid local gel formation during the process of hydrogel formation. In this scenario, the crosslinking density increased, and the steric exclusion grew so quickly that EDC could not access HA or SAL in that part of the hydrogel. Thus, the texture profile parameters decreased when the EDC/HA molar ratio was excessively high. In addition, a higher EDC/HA molar ratio resulted in the hydrogel having a smaller pore size (the SEM photographs are not shown in this article) that was not suitable for tissue scaffolding. In consideration of the hardness and cohesiveness, which are important factors in tissue engineering scaffolding, the recommended EDC/HA molar ratio was 4/1.

Swelling Capacity of the HA–SAL Hydrogels

The swelling capacity of the prepared hydrogels was evaluated by the determination of the swelling ratio. As with the texture characteristics, the swelling ratio can be used to evaluate the mechanical strength of a scaffold.[14] The swelling capacity, which is one of the most important properties for biomaterials, correlates with the infrastructure of biomaterials. The figure or morphology of biomaterials and also the cell amplification and differentiation (and even cell growth) may be influenced by the swelling capacity because of deformation from swelling. As shown in Figure 5(a), the equilibrium swelling ratios of the HA hydrogels were higher than those of the SAL hydrogels at a corresponding concentration because of HA's well-known high water absorption. Figure 5(a) also shows that in the HA hydrogels, the equilibrium swelling ratio of the sample at a lower concentration (0.5%) reached a steady value of 84.96; it reached only 28.63 at a higher concentration (1.5%). The swelling capacity of the hydrogels likely decreased because the steric exclusion grew with the increase in the concentration of HA. Because of the hardness of the hydrogels, in this study, we selected 1.0% as the material concentration.

Hydrogels with different HA/SAL molar ratios had different swelling capacities. Figure 5(b) shows that with decreasing HA in the HA/SA hydrogel, the equilibrium swelling ratio of the hydrogels declined. However, it increased with decreasing SAL. When the proportion of HA to SAL was 1:2 (the X value was 0.5), the swelling ratio reached 27%; this was similar to that of a hydrogel with 1.5% w/w single SAL. A lower swelling capacity could have reduced the material's influence on cell amplification and differentiation. Therefore, a composite hydrogel with a proportion of HA to SAL of 1:2 could be attractive for applications in tissue engineering scaffolds.

The effects of EDC on the swelling capacity were also examined. As shown in Figure 5(c), as EDC increased, the equilibrium swelling ratios of the samples declined. This indicated that

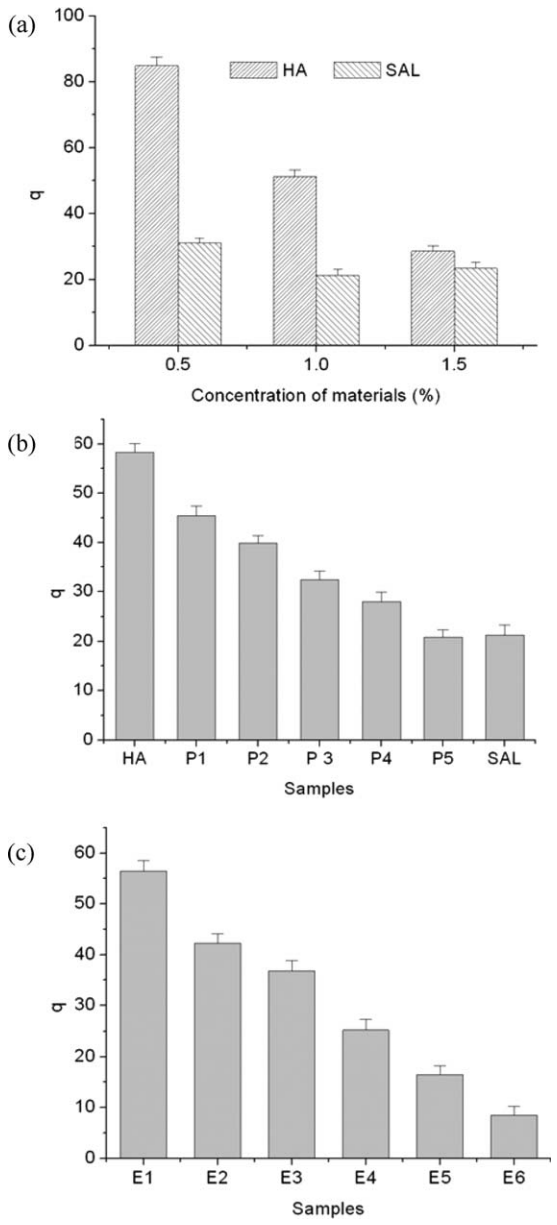

Figure 5. Characterization of the swelling capacity of the prepared hydrogels: (a) hydrogels with different concentrations of materials, (b) hydrogels with different molar ratios of HA to SAL, and (c) hydrogels with different molar ratios of EDC to HA.

denser networks lowered the water uptake capacity of the hydrogels. This occurred mainly because EDC and ADH were meant to create interhelical and intrahelical crosslinks and hold the helices together tightly.[32] The denser networks and smaller pore size of hydrogels led to a lower swelling capacity.

HAase Digestion *In Vitro* Testing of the Hydrogels

It has been reported that the degradation of HA is mainly caused by HAase, which is ubiquitous in human cells and serum.[8] As for the HA–SAL hydrogels used as tissue engineering scaffolding, resistance against HAase is crucial to their application. In particular for a cartilage tissue scaffold, the structure and figure must remain intact for about 14 days *in vitro* or

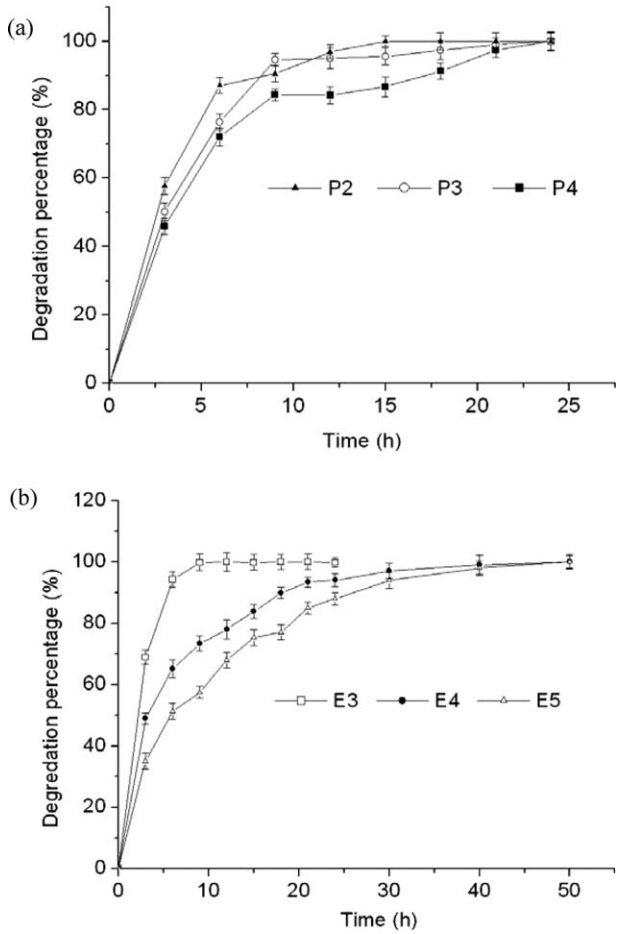

Figure 6. Resistance of the prepared hydrogels against HAase: (a) hydrogels with different molar ratios of HA to SAL and (b) hydrogels with different molar ratios of EDC to HA.

implantation *in vivo*.[33] In this study, the activity of HAase with 10 U/mL was selected; this was about 14 times higher than that of a typical injection (0.7 U/mL). Correspondingly, 24 h at the test level would be equivalent to 14 days of a typical usage level of HAase. We anticipated that the degradation progress would be completed in less than 48 h in our test. Figure 6 shows the kinetics of the degradation process. We found that the resistance of the hydrogels to HAase was negatively correlated with the proportion of HA [Figure 6(a)] and positively correlated with the EDC/HA molar ratio [Figure 6(b)]. As shown in Figure 6(a), almost all of the samples with different proportions of HA were degraded completely at 21 h. The degradation time could be prolonged over 30 h when more EDC was used [Figure 6(b)]. This indicated that when more HA was involved in the hydrogels, more interaction sites accessed the HAase. Additionally, when more EDC was used, much denser networks could be built; this greatly increased the steric exclusion against HAase attack.

CONCLUSIONS

A series of HA–SAL composite hydrogels was obtained through crosslinking by amide linkages. A suitable ratio between HA and SAL and the appropriate use of EDC resulted in a composite hydrogel with a regular porous network of ample size and improved hardness, springiness, and cohesiveness; this composite material may offer a biological environment conducive to cell attachment and proliferation. The equilibrium swelling ratio of the HA–SAL hydrogels was affected by the proportion of HA and the amount of EDC used. A lower swelling capacity was obtained when the proportion of HA and SAL was 1:2. With increasing SAL proportion and amount of EDC used in the reaction, the resistance against HAase was enhanced. Given the improved physicochemical properties that the composite HA–SAL hydrogels demonstrated, we conclude that they may have great potential for use in tissue engineering scaffolds.

ACKNOWLEDGMENTS

This work was supported by the Beijing Nova Program (contract grant number Z131105000413021) and the Foundation of the Chinese Academy of Agricultural Sciences for Outstanding Researchers.

REFERENCES

1. Bulpitt, P.; Aeschlimann, D. *J. Biomed. Mater. Res.* **1999**, *47*, 152.
2. Laurent, T. C. *Acta Otolaryngol.* **1987**, *442*(suppl), 7.
3. Weigel, P. H.; Hascall, V. C.; Tammi, M. *J. Biol. Chem.* **1997**, *272*, 13997.
4. Klauser, A. S.; Faschingbauer, R.; Kupferthaler, K.; Feuchnter, G.; Wick, M. C.; Jaschke, W. R.; Mur, E. *Eur. J. Radiol.* **2012**, *81*, 1607.
5. Song, M.; Kang, G. I.; Hwang, W. K.; Choi, W. G.; Kim, H. H.; Choi, W. C.; Ku, S. K.; Kwon, Y. S. *Toxicol. Lett.* **2011**, *205*, S238.
6. Kim, I. L.; Mauck, R. L.; Burdick, J. A. *Biomaterials* **2011**, *32*, 8771.
7. Pires, A. M. B.; Santana, M. H. A. *J. Appl. Polym. Sci.* **2011**, *122*, 126.
8. Collins, M. N.; Birkinshaw, C. *Carbohydr. Polym.* **2013**, *92*, 1262.
9. Liu, X.; Ma, P. X. *Ann. Biomed. Eng.* **2004**, *32*, 477.
10. Schanté, C. E.; Zuber, G.; Herlin, C.; Vandamme, T. F. *Carbohydr. Polym.* **2011**, *85*, 469.
11. Liu, L.; Liu, D. R.; Wang, M.; Du, G. C.; Chen, J. *Eur. Polym. J.* **2007**, *43*, 2672.
12. Hua, S.; Wang, A. *Carbohydr. Polym.* **2009**, *75*, 79.
13. El-Sherbiny, I. M. *Carbohydr. Polym.* **2010**, *80*, 1125.
14. Chung, C. W.; Kang, J. Y.; Yoon, I. S.; Hwang, H. D.; Balakrishnan, P.; Cho, H. J.; Chung, K. D.; Kang, D. H.; Kim, D. D. *Colloids Surf. B* **2011**, *88*, 711.
15. Grant, G. T.; Morris, E. R.; Rees, D. A.; Smith, P. J. C.; Thom, D. *FEBS Lett.* **1973**, *32*, 195.
16. Meera, G.; Abraham, T. E. *J. Controlled Release* **2006**, *114*, 1.
17. Vacanti, C. A.; Langer, R.; Sehloo, B. *Plast. Reconstr. Surg.* **1991**, *88*, 753.

18. Paige, K. T.; Cima, L. G.; Yaremchuk, M. J. *Plast. Reconstr. Surg.* **1995**, *96*, 1390.

19. Murata, Y.; Miyamoto, E.; Kawashima, S. *J. Controlled Release* **1996**, *38*, 101.

20. Ganesh, N.; Hanna, C.; Nair, S. V.; Nair, L. S. *Int. J. Biol. Macromol.* **2013**, *55*, 289.

21. Dahlmann, J.; Krause, A.; Möller, L.; Kensah, G.; Möwes, M.; Diekmann, A.; Martin, U.; Kirschning, A.; Gruh, I.; Dräger, G. *Biomaterials* **2013**, *34*, 940.

22. Oerther, S.; Payan, E.; Lapicque, F.; Presle, N.; Hubert, P.; Muller, S.; Netter, P. *Biochim. Biophys. Acta* **1999**, *1426*, 185.

23. Coates, E. E.; Riggin, C. N.; Fisher, J. P. *J. Biomed. Mater. Res. Part A* **2013**, *101*, 1962.

24. Chen, Y. H.; Wang, Q. *Carbohydr. Polym.* **2009**, *78*, 178.

25. Tomihata, K.; Ikada, Y. J. *Biomed. Mater. Res.* **1997**, *37*, 243.

26. Kuo, J. W.; Swann, D. A.; Prestwich, G. D. *Bioconjugate Chem.* **1991**, *2*, 232.

27. Huang, Y.; Onyeri, S.; Siewe, M.; Moshfeghian, A.; Madihally, S. V. *Biomaterials* **2005**, *26*, 7616.

28. Xia, W. Y.; Liu, W.; Cui, L.; Liu, Y. C.; Zhong, W.; Liu, D. L.; Wu, J. J.; Chua, K. H.; Cao, Y. L. *J. Biomed. Mater. Res. B* **2004**, *71*, 373.

29. Chang, C. H.; Liu, H. C.; Lin, C. C.; Chou, C. H.; Lin, F. H. *Biomaterials* **2003**, *24*, 4853.

30. Logeart-Avramoglou, D.; Anagnostou, F.; Bizios, R. *J. Cell. Mol. Med.* **2005**, *9*, 72.

31. Kang, J. Y.; Chung, C. W.; Sung, J. H.; Park, B. S.; Choi, J. Y.; Lee, S. J.; Choi, B. C.; Shim, C. K.; Chung, S. J.; Kim, D. D. *Int. J. Pharm.* **2009**, *369*, 114.

32. Nam, K.; Kimura, T.; Kishida, A. *Biomaterials* **2007**, *28*, 1.

33. Tortelli, F.; Cancedda, R. *Eur. Cell Mater.* **2009**, *30*, 1.